Available online at www.sciencedirect.com
SCIENCE DIRECT
Journal of Power Sources 156 (2006) 57–63
JOURNAL OF POWER SOURCES
www.elsevier.com/locate/jpowsour

Energy consumption reduction of a PEM fuel cell motor-compressor group thanks to efficient control laws

Mestan Tekin *, Daniel Hissel, Marie-Cécile Pera, Jean-Marie Kauffmann

Laboratory of Electrical Engineering and Systems (L2ES), UFC, UTBM Research Unit, UTBM, Bâtiment, F-90010 Belfort Cedex, France

Available online 25 October 2005

Abstract

This paper deals with the energy optimization of an embedded fuel cell generator. To reach this aim, experimentally validated models of a low power 5 kW proton exchange membrane fuel cell (PEMFC) and its most power hungry ancillary (motor-compressor group) are described. All simulation results have been performed using Matlab/Simulink® environment. Moreover, a control strategy of the air supply circuit integrated in an embedded fuel cell system is proposed. The air flow control of the air supply circuit is built around a fuzzy PD + I controller and for the air supply set point determination, a fuzzy supervision is proposed. The parameters of this fuzzy supervision have been optimized thanks to particle swarm optimization (PSO) method.

Keywords: Fuel cell system; Air supply circuit modeling; Fuzzy controller; Particle swarm optimization

1. Introduction

Currently, fuel cell vehicles are being developed as a potential alternative to conventional internal combustion engine vehicles. However, energy optimization of the complete fuel cell system still remains one of the most important technological bolts to be removed before seeing on the market commercial fuel cell vehicles. A fuel cell stack alone has good performance characteristics, but if the required air mass flow and air pressure rates are not reached, this performance will not be obtained in a vehicle application. Moreover, air supply circuit based on a motor-compressor group puts a great strain on the fuel cell system overall efficiency. Consequently, the optimization of the motor-compressor group and particularly its regulation strategy constitute a key milestone on the road of fuel cell vehicle development.

In a first part of this paper, special care is made on the embedded fuel cell system description and modeling. It is here made up on a 5 kW PEM fuel cell and its air supply circuit based on a motor-compressor group. Fuel cell and its air circuit models are validated respectively on a 5 kW fuel cell and a dedicated air compressor test bench. The second part of this paper proposes, for this embedded fuel cell system, a control strategy of the air supply circuit using fuzzy logic regulators. Two control loops are proposed: an internal air flow regulation loop and an air flow set point determination one. After description of the proposed fuzzy supervisor and the considered vehicle driving cycle, the PSO method will be presented and applied to reduce the energy consumption of the motor-compressor group. Finally, a comparison of simulation results obtained before and after the energy consumption optimization process will be presented.

2. Embedded fuel cell system modeling

2.1. Fuel cell generator

The fuel cell is an electrochemical device that produces directly electricity through the oxido-reduction reaction of hydrogen and oxygen. This generator is made up of a stack of single cells with an electrical series connection. In a hydrogen/air fuel cell, the electrical conversion net efficiency of the energy brought by the fuel is around 50%. This efficiency remains around this value in a very wide operating range, particularly for partial load operation, contrary to the conventional energy conversion systems. Among the different types of existing fuel cells, proton exchange membrane (PEM) fuel cells seem to be, to date, the best candidates for transportation applications. Contrary to the other types of fuel cells, PEM fuel cell has a solid electrolyte and its operating temperature is enough low (around

* Corresponding author.
E-mail address: mestan.tekin@utbm.fr (M. Tekin).

0378-7753/$ – see front matter © 2005 Elsevier B.V. All rights reserved.
doi:10.1016/j.jpowsour.2005.08.037

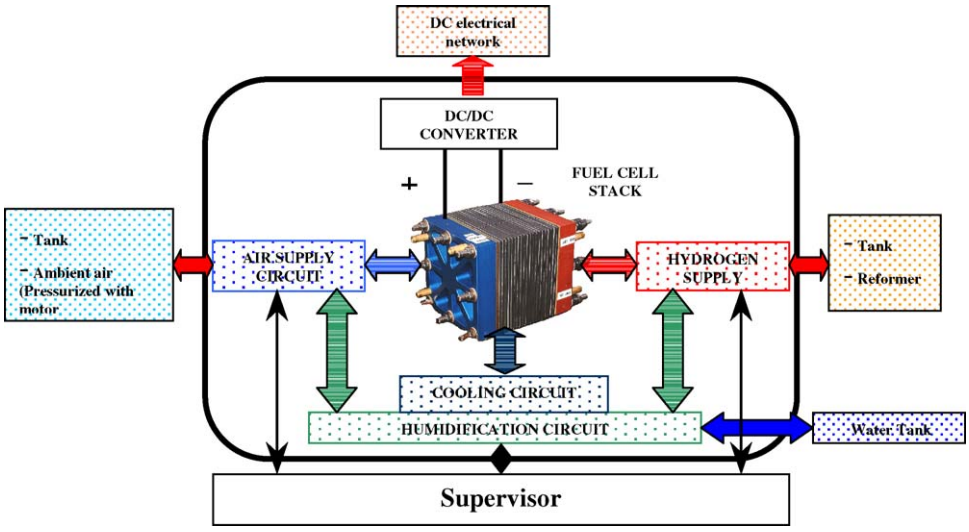

Fig. 1. Embedded PEM fuel cell generator.

80 °C) allowing an fast starting of the embedded fuel cell generator [1].

To ensure its correct operation, PEM fuel cell is surrounded by a lot of ancillary circuits. The generator constituted by the fuel cell stack and its ancillaries is called the fuel cell system. In such a system, there are generally four ancillary circuits (Fig. 1):

- Cooling circuit: It allows evacuating heat produced by the electrochemical reaction. A water-cooling circuit seems necessary for fuel cell above 500 W. This circuit consumes usually about 3% of the available electrical stack power.
- Humidification circuit: In order to maintain the membrane in a correct state of hydration (to ensure protons transfer), this circuit allows humidification of gases (hydrogen and air) that enter the fuel cell stack permanently. It consumes up to 5% of the available electrical stack power.
- Hydrogen and air supply circuits: These circuits allow supplying stack anodic and cathodic compartments with hydrogen and air (oxygen). In the simplest case, hydrogen is directly stored in high pressure cylinders (from 300 to 700 bars) onboard vehicle and hydrogen flow can be regulated by a reducing pressure valve according to its consumption. In this case, hydrogen supply circuit consumes only less than 2% of the available electrical power of the stack. Experimental tests on fuel cells underline the fact that electrochemical conversion efficiency is much higher at high partial pressures [2]. Moreover, the regulation of the power delivered by the fuel cell implies an efficient regulation of the oxygen incoming flow. These two facts justify the use of a variable speed (air flow) motor-compressor group for the air supply circuit. Nevertheless, currently used motor-compressor groups consume up to 25% of the available electrical energy at the output of the stack.

So, all these ancillary circuits put a great strain on the overall system efficiency. Among them, air supply circuit based on a motor-compressor group is the most power-hungry. It represents up to 80% of consumption of the overall ancillaries. Consequently, in order to perform both the energy optimization and the energy control of an embedded fuel cell system, it seems judicious to investigate and model firstly the air supply sub-system.

2.2. Fuel cell modeling

Single cells are supposed to be identical; they also have the same behavior. Moreover, the distribution of the current density is supposed to be uniform. Consequently, the fuel cell stack is modeled like a single cell. In the very simple considered fuel cell model, only output voltage and pressure drop in cathode compartment are evaluated. Fuel cell output voltage depends on the current density (J), stack temperature (T), partial pressures of oxygen and hydrogen gases on catalytic sites (P_{O_2}, P_{H_2}) according to (1) [3].

$$U = U_0 + \alpha T \ln(P_{O_2}) + \beta T \ln(P_{H_2}) + \gamma T + \delta T \ln(J) - rJ \quad (1)$$

U_0, α, β, γ, δ and r are the coefficients identified from experimental tests carried out on the 5 kW test bench (Fig. 2). This fuel cell stack is composed of 40 single cells, and each one has a surface of 400 cm^2. The fuel cell rated current is 180 A with a rated voltage around 27 V. Operating temperature is 55 °C. Fig. 3 represents the simulated and measured polarisation curves of our 5 kW fuel cell.

On the 5 kW fuel cell test bench, cathode and anode compartment outlet pipes were equipped with pressure reducing valves to make it possible to carry out the tests with various operating pressures. So, from the fuel cell air outlet pressure, it is possible to evaluate the air inlet pressure (pressure delivered by the motor-compressor group) by a simple Darcy–Weisbach relation as following [4]:

$$\Delta P_{cat} = \frac{1}{2} L_{cell} F_{SC} \rho_{air} \frac{\Lambda(Re)}{HD} \left(\frac{q_{m_{air}}}{A_{cat}} \right)^2 \quad (2)$$

Fig. 2. Five kilowatts fuel cell test bench in the laboratory.

ΔP_{cat} is the pressure drops in cathode compartment of the fuel cell, L_{cell} the length of cathodic side distribution channels, F_{SC} the stoichiometric factor of the cathode compartment, ρ_{air} the air mass density, $\Lambda(Re)$ the coefficient depending on the flow nature (Reynolds number) and the friction inside the cell, HD the hydraulic diameter, $q_{m_{air}}$ the inlet air flow (with oxygen depletion according to the fuel cell current) and A_{cat} is the transversal section of cathodic side distribution channels.

2.3. Air supply sub-system modeling

Despite the many different types of compressor technologies available on the market, a rotary vane compressor has been chosen. Indeed, the low rotational speed of these compressors (less than 5000 rpm) makes it possible to avoid lubrication and implies also a simpler construction and a lower cost. Thus, for the motor-compressor group, a rotary vane compressor especially developed for fuel cell applications (provided by Vairex Corp.) and a brushless dc motor have been chosen.

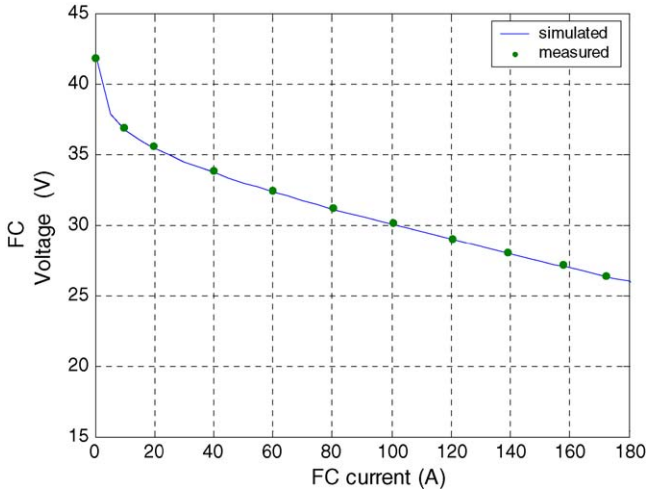

Fig. 3. Five kilowatts fuel cell polarisation curve (U–I) with T=55 °C and $P_{cathode}$ = 1.8 bar.

Characteristics of the chosen motor-compressor group dedicated to supply the 5 kW PEM fuel cell are the following:

- air quality: oil free (fuel cell generator lifetime is reduced by residual oil droplets presence in air inlet);
- maximum mass flow: 15 g s^{-1} (corresponds to a maximum current of 300 A with an air stoichiometry of up to 3);
- maximum absolute outlet pressure: 1.5 bars;
- rated rotational speed: 2800 rpm;
- rated power: 860 W;
- electromechanical time constant of the motor: 2 ms.

Rotary vane compressor is composed of a cylinder and a rotor which turns around an off-center axis in this cylinder. This rotor is equipped with radial vanes, which freely slide and are constantly applied to cylinder wall. Thus, the volume between two consecutive vanes is variable and air compression is obtained by decreasing of this variable volume. So, rotary vane compressor modeling (developed in Matlab/Simulink® environment) consists in evaluating the compressed air quantity for each rotor revolution. So, this model is constituted of four inputs (rotational speed, inlet air temperature, inlet and outlet air pressures) and four outputs (air mass flow, air outlet temperature, compressor torque and mechanical power). Parameters used for modeling are the compressed volume per revolution ($V_{comp/r}$) obtained thanks to the compressor dimensions, air heat capacity (c_p) and air masse constant (r_{air}).

The expression of air mass flow (q_m) is depending on rotational speed (ω) of compressor according to [5]:

$$q_m = \frac{1}{2\pi}\eta_{vol}\rho_{air}V_{comp/r}\omega \tag{3}$$

with η_{vol} is the volumetric efficiency of rotary vane compressor and ρ_{air} is the air inlet mass density.

Another part of compressor model is the evaluation of power consumption. In fact, the compressor power is depending on the pressure ratio and the mass flow [6]:

$$P_{comp} = \frac{q_m c_p T_i}{\eta_{ad}\eta_{mec}}\left(\left(\frac{P_0}{P_i}\right)^{(\gamma-1)/\gamma} - 1\right) \tag{4}$$

γ term is the isentropic coefficient (γ = 1.4 for air), η_{ad} the adiabatic efficiency of the rotary vane compressor depending on compressor load conditions (frictions, heat transfers) and η_{mec} is the mechanical efficiency of the rotary vane compressor.

Brushless dc motor is modeled with the equivalent Park machine which allows simplifying motor equations. Inputs of this model are the three phase voltages coming from the inverter and the compressor load torque. The outputs of this model are the consumed electrical power and the motor-compressor group rotational speed.

Fig. 4 compares simulation an experimental results (when static conditions have been reached) of the power consumed by motor-compressor group for different outlet pressure ratios (r_p) and Fig. 5 shows the responses (in p.u.) of the air compressor speed and mass flow to a step solicitation. As it can be seen on these figures, experimental and simulation results are in

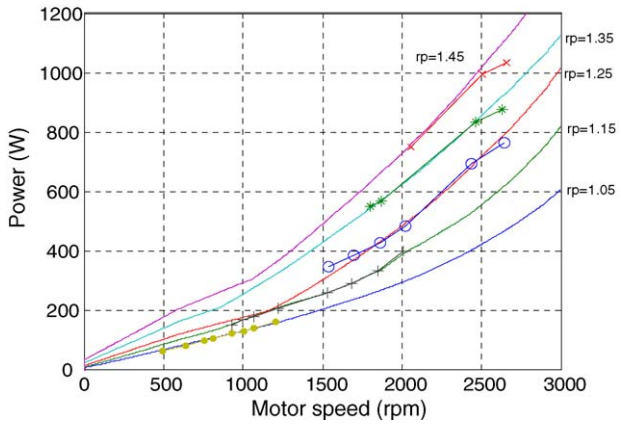

Fig. 4. Power consumed by the motor-compressor group.

perfect adequacy for both the speed and the obtained air mass flow.

2.4. Traction motors modeling and considered vehicle driving cycle

The considered vehicle traction system is composed of four identical speed regulated wheel-dc motors supplied with a direct current converter. The maximum power of each one of these motors is about 10 kW with a maximum rotational speed of 1500 rpm and the speed reference is imposed from driving cycle according to the sizes of the wheels. However, in order to make possible the connection with the 5 kW fuel cell generator, direct current converters are connected to the vehicle dc electrical network by applying a normalization factor of one-tenth on the consumed power value of vehicle traction system.

The complete model of the embedded fuel cell system (composed of the 5 kW fuel cell stack model, the air supply circuit model and the vehicle traction motors model) is tested on a vehicle driving cycle provided from the vehicle simulator program: Advisor® (profile name: "CYC_UDDS-Urban Dynamometer Driving Schedule", Fig. 6).

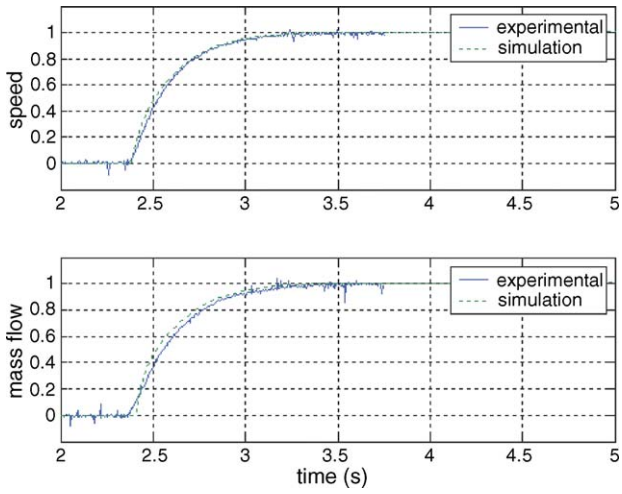

Fig. 5. Normalized compressor speed and air mass flow.

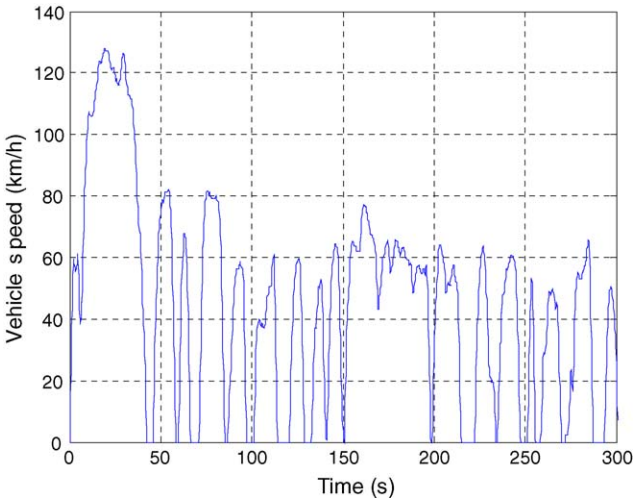

Fig. 6. Vehicle speed profile from Advisor® (CYC_UDDS).

Simulations were carried on first minute of this driving cycle. Moreover, after 35 s of this driving cycle, a water plug fault was added on the fuel cell stack model. Indeed, water plug in cathode compartment occurs frequently on PEM fuel cell especially for long operating time of the stack. This fault produces a rapid stack voltage drop.

3. Embedded fuel cell system control strategy

The control strategy of the air supply circuit in embedded fuel cell system is essential for its correct operation. Indeed, fuel cell ancillaries are not independent sub-systems and they are supplied by the fuel cell itself via vehicle dc electrical network. Moreover, in transportation applications, energy sources are requested in a very wide operating range and vehicle performances are directly correlated to the energy source's dynamical response. However, embedded fuel cell generators are able to provide requested power almost instantaneously, as long as they have sufficient quantity of gases. So, to avoid reducing lifetime of the fuel cell, control strategy of the motor-compressor group must be able to respond to dynamic fuel cell current solicitations. For example, during an increase of power requested by the vehicle, the motor-compressor group must also increase the fuel cell inlet air flow accordingly. As air and hydrogen gas flows increase, the humidification circuit must react quickly enough to avoid the drying of the membrane. Moreover, the cooling circuit must maintain fuel cell temperature in its operating range and the fuel cell voltage must be monitored to avoid gas diffusion limitation problems.

The motor-compressor group control strategy proposed in this paper is composed of two loops: the first one is dedicated to the internal air flow regulation of the motor-compressor group. The second one is dedicated to the air flow set point determination. For implementation of these two regulation loops, non-linear Takagi–Sugeno fuzzy logic controllers have been used. Indeed, fuzzy logic controllers are very robust, because they are tolerant to imprecise measurements and to component variability. Moreover, this type of fuzzy controller is suitable for real time control on vehicle applications.

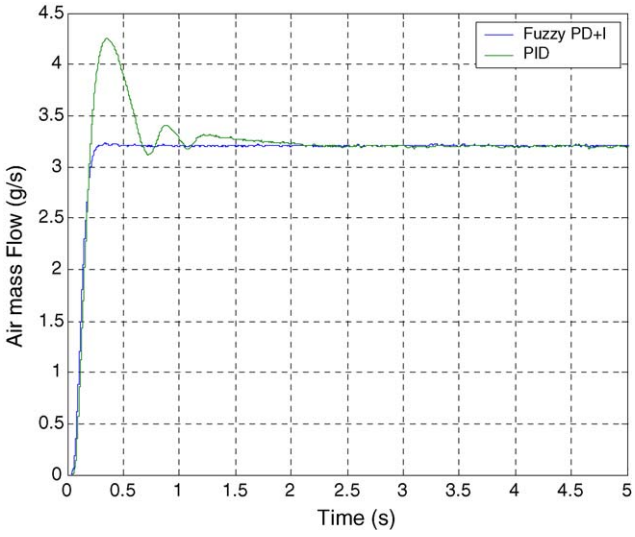

Fig. 7. Motor-compressor group air mass flow response obtained with traditional PID and fuzzy PD + I controller.

3.1. Internal air flow regulation loop

In order to regulate and supply the required air quantity with an acceptable response time to the fuel cell stack, we proposed for internal air flow regulation loop a non-linear fuzzy PD + I regulator [7]. This regulator is called PD + I because only its proportional and derivative parts use fuzzy logic. Moreover, in order to set the air flow dynamic to be respected by the regulator, a rise time value of 135 ms was defined. This value has been obtained according to the oxygen volume that is present inside the cathode compartment and the time during which this oxygen can supply the 5 kW fuel cell in case of a nominal current solicitation [8].

Figs. 7 and 8 compare experimental results obtained with our fuzzy PD + I regulator and with a traditional PID regulator on the motor-compressor group for the same air flow rising time value. The fuzzy PD + I controller presents the same behavior as the conventional PID controller, but without overshoot. Moreover, if the energy consumption of the two solutions is compared for the same rising time, the fuzzy non-linear solution leads to about 8% reduction of energy consumption after 5 s of test.

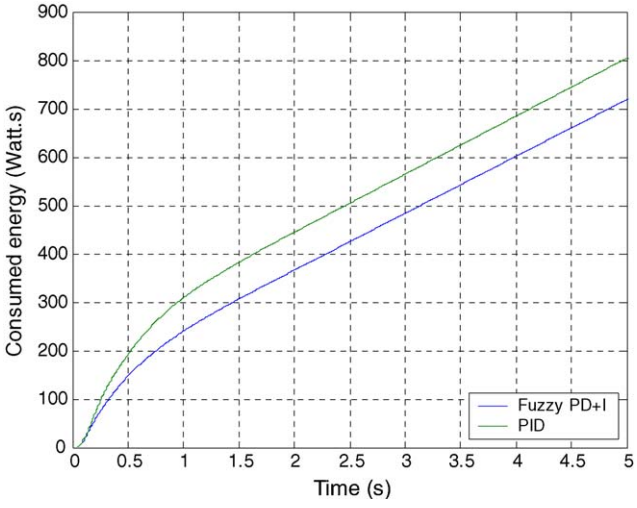

Fig. 8. Cumulated energy consumed by the motor-compressor group with traditional PID controller and fuzzy PD + I controller.

3.2. Evaluation of the required air quantity

Evaluation of the required air quantity is carried out according to the current requested from the dc electrical network, which is the sum of currents consumed by the vehicle traction motors, by vehicle electrical auxiliaries (light, turn signal lamp, air conditioning system, etc.) and by fuel cell ancillaries. In our case, only the motor-compressor group current (which represents up to 80% of the consumption of the fuel cell ancillaries), was added on dc electrical network. The determination of the air flow reference is also depending on the fuel cell voltage. Indeed, by increasing air flow over its real consumption in the stack, partial pressure of oxygen will increase in cathode compartment. This overpressure will then increase fuel cell voltage (1).

The determination of air flow set point is carried out thanks to a fuzzy type supervisor which is based on five inputs: fuel cell voltage, fuel cell voltage derivative, fuel cell current, fuel cell current derivative, fuel cell requested power derivative and one output: air flow [9].

Fig. 9 represents fuel cell voltage curves before and after supervision of the considered embedded fuel cell system. It can be noticed that, on the one hand, without fuzzy supervision, the fuel cell voltage decreases dramatically and may cause the destruction of the fuel cell. On the other hand, with fuzzy supervision, air compressor increases quickly the air flow to drain water droplet in cathode compartment. Fig. 10 compares cumulated energy delivered by the fuel cell stack to the system (traction + air supply ancillary). During complete cycle, only 2% more energy is used by motor-compressor group with fuzzy supervision (including fault management). Nevertheless, it results in an energy consumption increase. Therefore, in order to reduce the consumed energy by the air supply circuit, an optimization process of the fuzzy logic supervisor parameters must be performed.

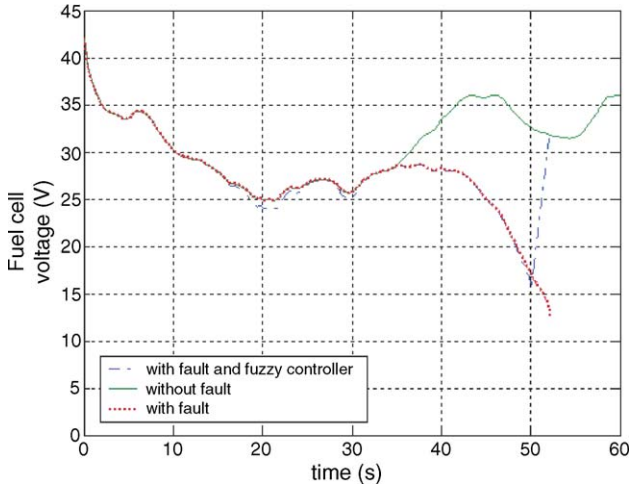

Fig. 9. Fuel cell voltage curves.

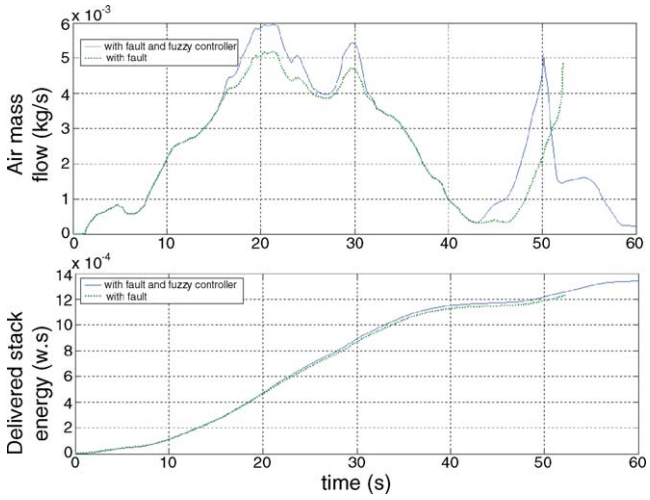

Fig. 10. Air mass flow and cumulated energy delivered by the fuel cell stack.

4. Energy optimization

In order to reduce air supply circuit energy consumption and thus to increase fuel cell system overall efficiency, optimization of the fuzzy supervisor parameters (16 parameters) was carried out with particle swarm optimization (PSO) algorithm. Unlike genetic algorithms, PSO has no evolution operators such as crossover and mutation. Its main advantages are that PSO algorithm is easy to implement and there are few parameters to adjust. At present time, PSO has been successfully applied in function optimization, artificial network training and optimization of fuzzy system parameters [10].

4.1. Particle swarm optimization

PSO like genetic algorithms is a population-based evolutionary computation technique. It differs in that each particle (or agent) of the population has a position and velocity. PSO uses a principle of social behavior of a group like bird flocking and fish schooling. A group can effectively achieve an objective by using the common information of every agent and the information owned by the agent itself [11].

For example, we consider the scenario of a group of birds randomly looking for food in an area [12]. If one member of birds flock lands to a source of food, other members will modify their flight directions and tend to converge around the successful individual, increasing their own chances of success. Indeed, PSO algorithm consists in modeling the exploration of the problem space by a population of particles. All of particles have a fitness value which is evaluated by a fitness function. Like in other evolutionary optimization method, the population of individuals is updated by applying some operators according to the fitness information so that the individuals can be expected to move toward better solution areas.

Firstly, PSO is initialized with randomly positioned group agents. Each agent is treated as a point in a D-dimensional space and represented with its position ($x_i = (x_{i1}, x_{i2}, \ldots, x_{iD})$) and velocity ($v_i = (v_{i1}, v_{i2}, \ldots, v_{iD})$). Only its best previous position ($p_i = (p_{i1}, p_{i2}, \ldots, p_{iD})$) that gives its best fitness value and the best agent position ($p_g = (p_{g1}, p_{g2}, \ldots, p_{gD})$) among all the population are memorized. At every iteration, the agent dynamics is governed by the following equation which updates its positions and velocities:

$$v_i(k+1) = \chi[v_i(k) + \mathrm{rand}(0, \varphi_2)(p_i - x_i(k)) + \mathrm{rand}(0, \varphi_2)(p_g - x_i(k))] \quad (5)$$

$$x_i(k+1) = x_i(k) + v_i(k+1) \quad (6)$$

Coefficient χ is the constriction factor, which depends on φ_1 and φ_2:

$$\chi = \begin{cases} \dfrac{2\kappa}{\varphi - 2 + \sqrt{\varphi^2 - 4\varphi}} & \text{for } \varphi < 4 \\ \sqrt{\kappa} & \text{for } \varphi < 4 \end{cases} \quad \text{with } \varphi = \varphi_1 + \varphi_2 \quad (7)$$

These coefficients determine the relative influence of the social learning rate and cognitive components. Eqs. (5) and (6) are used to calculate the agent's new velocity according to its previous velocity, the distances of its current position from its own best position and the group's best position. Then, the agent flies toward its new position. This PSO algorithm will continue until a minimum error criterion is attained or the number of iterations defined by user is reached.

The particles number in the swarm was set to 80 and the maximum number of iterations to 200. All particles will fly through a 16-dimensions space where each dimension has different limits. According to the particles positions, the fitness function to be minimized is calculated by the ratio of the energy consumed by the motor-compressor group to the delivered fuel cell energy at the end of the considered driving cycle:

$$f = \frac{\int_t P_{\mathrm{comp}}\,\mathrm{d}t}{\int_t P_{\mathrm{FC}}\,\mathrm{d}t} \quad (8)$$

with P_{comp} and P_{FC} are the powers consumed by the motor-compressor group and delivered by the fuel cell stack to the dc electrical network. Moreover, some limit conditions on the fuel cell minimum voltage value (>0.35 Ufc), fuel cell maximum current value (<250 A) and air stoichiometry factor value were added beside this fitness function.

4.2. Optimization results

A first optimization was carried out while maintaining air stoichiometry factor condition higher than 2. This value of air stoichiometry is recommended by the 5 kW fuel cell manufacturer and respected during simulations before optimization. Then, in order to evaluate air stoichiometry effect on motor-compressor group energy consumption, a second optimization was carried out while reducing the constraint of air stoichiometry factor to 1.

During the second optimization process, air stoichiometry factor decreases up to 1.5. The ratios between the motor-compressor energy consumption and the energy delivered by

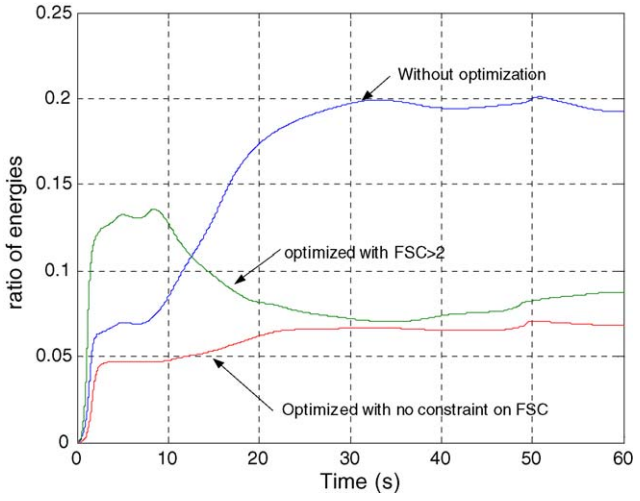

Fig. 11. Ratio between the consumed energy by motor-compressor group and energy delivered by fuel cell before and after optimization.

the fuel cell to the system (fitness function) before and after optimizations are presented in Fig. 11. It can be shown in this figure that the energy consumption reduction is very significant. Indeed, at the end of the considered vehicle driving cycle, results of the fitness function reduces from 0.18 to 0.08 for the first optimization, and to 0.07 for the second optimization.

5. Conclusion

This article proposes fuzzy logic control solutions for the motor-compressor group supplying an embedded PEM fuel cell system.

The first part on this paper is dedicated to the description of an embedded fuel cell generator. The experimentally validated models of a 5 kW fuel cell and its air supply circuit are detailed. Moreover, vehicle traction motors model and its driven cycle are respectively presented. The second part proposes a control strategy of the air supply sub-system allowing harmonization of the stack and fuel cell ancillaries' behaviors facing system faults. This strategy is based on a two fuzzy logic fuzzy controllers. In the last part, PSO method has been chosen to obtain optimal values for the proposed fuzzy logic supervisor parameters. So, a detailed principle of the PSO is presented. Finally, simulation results obtained before and after optimizations have been compared.

References

[1] M.C. Péra, D. Hissel, J.M. Kauffmann, Fuel cell systems for electrical vehicles: an overview, IEEE VTS News 49 (1) (2002) 9–14.
[2] A. Wiartalla, S. Pischinger, W. Bornscheuer, K. Fieweger, J. Orgzewalla, Compressor Expander Units for Fuel Cell Systems, Institute for Combustion Engines, FEV Motorentechnik GmBH, Aachen, 2000.
[3] J.C. Amphlett, R.M. Baumert, R.F. Mann, B.A. Peppley, P.R. Roberge, T.J. Harris, Performance modeling of the ballard mark IV solid polymer electrolyte fuel cell. I. Mechanistic model development, J. Electrochem. Soc. 142 (1) (1995) 1–8.
[4] D. Hissel, M.C. Péra, X. François, J.M. Kauffmann, P. Baurens, Contribution to the modelling of automotive systems powered by polymer electrolyte fuel cells, in: Proceeding of the Eighth European Automotive Congress, Bratislava, 2001, pp. A319–A326.
[5] M. Tekin, D. Hissel, M.C. Pera, J.M. Kauffmann, Energy optimization of an embedded fuel cell system using particle swarm, in: IEEE Vehicle Power and Propulsion 2004 (VPP'04), Paris, October 2004 (CD-ROM).
[6] D. Boettner, G. Paganelli, Y. Guezennec, M.J. Moran, Proton exchange membrane fuel cell system model for automotive vehicle simulation and control, J. Energy Resour. Technol. 124 (2002) 20–27.
[7] D. Hissel, Contribution à la commande de dispositifs électrotechniques par logique floue, PhD, INPT, Toulouse, France, 1998.
[8] M. Tekin, D. Hissel, M.C. Péra, J.M. Kauffmann, Energy optimization of a fuel cell generator: modelling and experimental results, in: Proceedings of the EPE'2003 Conference, Toulouse, France, 2003 (CD-ROM).
[9] M. Tekin, D. Hissel, M.C. Pera, J.M. Kauffmann, Energy management strategy for embedded fuel cell system using fuzzy logic, in: Proceedings of the IEEE International Symposium on Industrial Electronics (ISIE'04), Ajaccio, May, 2004, pp. 501–506.
[10] A.A.A. Esmin, A.R. Aoki, G. Lambert-Torres, Particle swarm optimization for fuzzy membership functions optimization, in: Proceedings of the IEEE International Conference on Systems, Man and Cybernetics, 2002, pp. 108–113.
[11] J. Kennedy, R.C. Eberhart, Particle swarm optimization, in: Proceedings of the 1995 IEEE International Conference on Neural Network, vol. 4, 1995, pp. 1942–1948.
[12] Y. Shi, Particle swarm optimization, IEEE Neural Netw. Soc. Mag. (2004) 8–13.